

Calculation of excited states via symmetry constraints in the Variational Quantum Eigensolver

Gabriel Greene-Diniz

David Muñoz Ramo

Cambridge Quantum Computing Ltd.

9a Bridge Street, CB2 1UB Cambridge

United Kingdom

May 6, 2022

Abstract

The variational quantum eigensolver (VQE) algorithm, designed to calculate the energy of molecular ground states on near-term quantum computers, requires specification of symmetries that describe the system, e.g. spin state and number of electrons. This opens the possibility of using VQE to obtain excited states as the lowest energy solutions of a given set of symmetries. In this paper, the performances of various unitary coupled cluster (UCC) ansätze applied to VQE calculations on excited states are investigated, using quantum circuits designed to represent single reference and multireference wavefunctions to calculate energy curves with respect to variations in the molecular geometry. These ansätze include standard UCCSD as well as the recently developed UCCGSD and k -UpCCGSD which are engineered to tackle the calculation of states with strong multireference character. These studies are carried out on H_2 , H_3 , and the methylene radical CH_2 as examples of molecules with spin singlet, doublet and triplet ground states respectively, at different spin configurations and charge states. In most cases, our calculations for all states considered are in excellent agreement with results from full configuration interaction calculations on classical machines, thus showing that the VQE algorithm is capable of calculating the lowest excited state at a certain symmetry, by setting appropriate constraints in the qubit register encoding the starting mean field state. In the case of the CH_2 calculations using the k -UpCCGSD ansätze, calculations result in up-shifted spin singlet states relative to the FCI limit. Comparing the optimized cluster amplitudes between k -UpCCGSD and UCCGSD, the lack of some generalized double excitations in k -UpCCGSD accounts for the increased energy of the first singlet excited state relative to UCCGSD. In addition, we observe spin crossover between different spin states when using generalized ansätze, which can be prevented by the use of penalty terms in the hamiltonian and qubit registers encoding multireference states. Comparison of calculations with qubit registers encoding different types of CH_2 singlet states (closed-shell and open-shell) suggest that conventional VQE may be able to calculate higher energy excited states beyond the first one for a particular set of symmetries, although with a significant loss in accuracy of the results.

1 Introduction

The theoretical elucidation of the energy and properties of molecules and materials at the atomistic level has been identified for a long time as one of the most straightforward applications of quantum computing. This assessment is motivated by the relatively low requirements of the corresponding quantum circuits in comparison with other applications [1]. The use of quantum computers for atomistic simulations promises to bring radical advances in a variety of fields including pharma, photovoltaics, aeronautics, electronics and energy generation, among others. Most research efforts have been focused on efficient algorithms for the calculation of the molecular ground state energy, although in recent years work has been performed in the calculation of other quantities like excited state energies [2–5] or energy derivatives [6–8].

Current quantum computers display high levels of noise at different stages of their operation, and it is expected that near-term machines will continue having to grapple with this problem [1]. Motivated by this fact, a variety of hybrid quantum-classical algorithms based on the Variational

Quantum Eigensolver (VQE) [9] have been proposed over the years. VQE's main advantage relies on its improved resiliency to noise and reduced circuit depth compared with pure quantum algorithms like quantum phase estimation. Since VQE's inception, many improvements have been proposed: schemes to simplify and generalize the wavefunction ansatz [10–14], techniques to reduce the impact of noise in the quantum circuit [15] or in the classical minimization step [16, 17] or strategies to reduce the number of measurements of the hamiltonian [18, 19], among others. A comprehensive review of these techniques may be found in Refs. [20, 21].

VQE is designed to calculate the energy of molecular ground states, as the variational nature of the algorithm drives the calculation to the minimum of the energy function. The calculation typically starts by encoding a mean-field wavefunction obtained by a classical calculation with techniques like the Hartree-Fock method. In the second quantization formalism, the qubit register represents the occupations of the molecular spin orbitals. However, encoding the mean-field wavefunction into a qubit register is associated with defining some symmetries that describe the molecular system, such as the number of electrons or the spin state. One could perform experiments in which there is a selection of symmetries corresponding to states different from the ground state, for example setting the spin state of the qubit register to a triplet in the hydrogen molecule. These symmetries would constrain the wavefunction to drive the VQE algorithm towards local energy minima that satisfy them, effectively transforming this algorithm into a tool to determine the lowest excited state compatible with a given symmetry. Recent work by other authors suggests that this strategy is bound to fail and VQE should always converge to the global energy minimum at a given geometry. However, for this analysis the VQE approach was based on the variational optimization of the mean-field function on the quantum processor, in addition to the optimization of the ansatz parameters [16, 22], which implies removing symmetry constraints from the calculation.

Studying excited states with VQE leads to another possible complication. Molecular excited states usually display higher entanglement than ground states and a mean-field trial wavefunction is a bad starting point for a correlated calculation on these systems. In quantum chemistry, these states are referred to as multireference states, alluding at the fact that more than one reference state is needed to properly describe entanglement in these systems. It is well documented in the literature that conventional coupled cluster methods fail to obtain the appropriate description of multireference states [23, 24], and need to be adapted for these cases. In this sense, it is interesting to investigate the performance of VQE with the standard UCCSD ansatz in the calculation of these kinds of problems. Recently, advanced ansätze have been proposed which have been engineered to tackle the calculation of states with strong multireference character [10, 11]. Their accuracy in the case of excited states is also interesting to assess.

In this paper, we explore these questions by applying VQE to a series of molecules with different choices for the starting Hartree-Fock wavefunction and the correlation ansatz. The simplest system analyzed is H_2 , which is representative of molecules with a closed-shell singlet ground state and a triplet excited state. For the doublet case, we choose H_3 in a linear geometry as the simplest system to analyze. Finally, we look at the methylene radical, CH_2 , whose ground state is a spin triplet with two unpaired electrons and its lowest excited states are spin singlets with strongly entangled character. CH_2 is well known in the chemistry community as a good model for the study of electron correlation in excited states [25, 26]. In the context of quantum computing, it has already been used as a test molecule for the study of adiabatic state preparation and phase estimation techniques [5, 27]. We follow the lead of these studies and propose CH_2 as a good test molecule for the study of the treatment of entanglement in quantum chemistry for quantum computing. We start by explaining the methodology used for the calculations. We then follow by showing our results for the H_2 and H_3 molecules. Next, we study the case of CH_2 . We finalize our study with a discussion of the results obtained.

2 Methods

All the calculations have been performed using our EUMEN quantum chemistry package in combination with the ProjectQ quantum simulator [28] and auxiliary functions provided by the Open-Fermion library [29]. Our calculations required the computation of molecular integrals to define the second quantization hamiltonian. This step was done with the Psi4 package [30], which was also used to perform Full Configuration Interaction (FCI) and classical CCSD and EOM-CCSD calculations for comparison purposes.

We used different basis sets and active spaces depending on the species considered. For H_2 and

Molecule	Initial wavefunction qubit register
H_2 (6-31G)	$ 11000000\rangle$ (S) $ 10100000\rangle$ (T)
H_3 (6-31G)	$ 111000000000\rangle$ (D) $ 101010000000\rangle$ (Q)
CH_2 (STO-3G)	$ 11110100000\rangle$ (T) $ 111111000000\rangle$ (S1) $\frac{1}{\sqrt{2}} 111111000000\rangle - \frac{1}{\sqrt{2}} 111100110000\rangle$ (S2) $\frac{1}{\sqrt{2}} 111101100000\rangle - \frac{1}{\sqrt{2}} 111110010000\rangle$ (S3)

Table 1: Initial state qubit encoding for H_2 , H_3 and CH_2 at different spin symmetries. The alternating spin-up/spin-down convention is used for the spin orbital occupations encoded in the qubit registers. Letters between brackets refer to spin multiplicities: S (singlet), D (doublet), T (triplet), Q (quadruplet). For CH_2 , three different spin singlets are considered: S1, S2 and S3.

H_3 , we used the 6-31G basis set in order to be able to correlate the high-spin wavefunctions. This basis is prohibitively expensive to use in a simulator for CH_2 . Therefore, we resorted to a STO-3G basis set with the 1s C core orbital frozen to reduce the size of the qubit register needed for the simulations. This setup is enough to capture the effects of correlation at different spin states for this molecule.

For these calculations we used the VQE algorithm with the regular UCCSD ansatz (adapted for open-shell configurations). In addition, the advanced ansatz k -UpCCGSD [10] was applied to calculate several geometry points for CH_2 . In this ansatz, virtual-virtual and occupied-occupied excitation operators are included in the cluster operator expression, and double excitations where electron pairs do not have the same spatial orbital are skipped. Some calculations were also done with the UCCGSD ansatz [10], where all excitations are considered, and in these cases only a few points of the energy curve were calculated due to the large computational expense associated with the fully generalized cluster operator. Encoding of the Hamiltonian and the wavefunction was performed using the Jordan-Wigner scheme. The Bravyi-Kitaev [31] scheme was also tested for the ground and first excited state of CH_2 , and no significant difference was observed relative to the Jordan-Wigner scheme.

As initial states, we first considered qubit registers encoding open shell multiplets and closed shell singlets from a Hartree-Fock calculation created by applying X gates to the qubits representing the occupied Hartree-Fock molecular orbitals. Different charge states are also considered. For the CH_2 case, we considered two initial entangled states representing multireference open-shell and closed shell singlet wavefunctions in addition to the closed-shell singlet wavefunction constructed from a single Slater determinant. We will refer to them as S3 (see the Appendix), S2 and S1, respectively. We designed small quantum circuits to prepare these states, which we show in Figure 1. These circuits act on qubits 4 to 7 of the register, corresponding to the sp hybridized valence shell and closest virtual orbitals of CH_2 . Qubits 0 to 3 are prepared as previously explained by applying X gates to represent the occupied spin orbitals below the valence shell of CH_2 . The details of the qubit registers encoding the wavefunctions for all the molecules considered are shown in Table 1.

3 Results

We summarize here our experiments with VQE ran over three different systems at several spin and charge states.

3.1 VQE results for H_2 and H_3

We begin our analysis with an evaluation of the energy curves of the H_2 molecule at different bond lengths. The ground state of this molecule is a spin singlet, and its first excited state has triplet symmetry. Our singlet calculation, as expected, has a good match with the singlet energy curve calculated with classical methods. In addition, our calculation of the triplet state at the 6-31G level, using the T initial Hartree-Fock encoding shown in Table 1, yields an energy curve that also

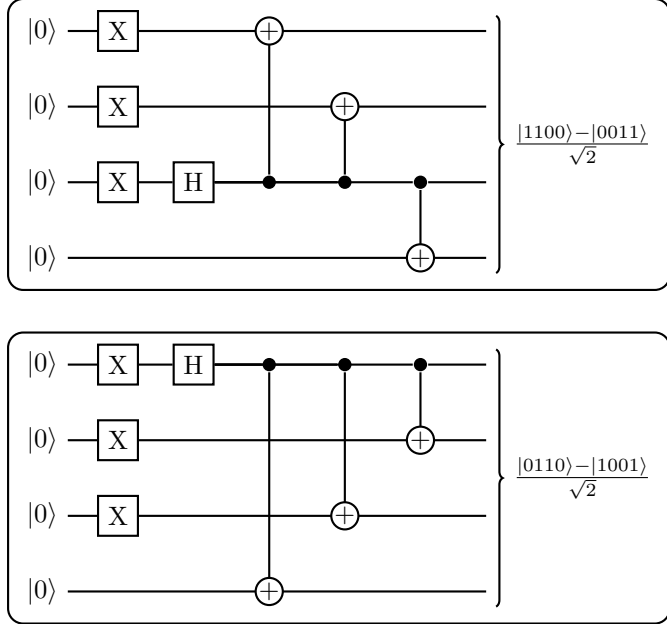


Figure 1: Circuit diagrams for the preparation of the multiconfigurational states consisting of a linear combination of closed-shell (top panel) or open-shell (bottom panel) singlets for the CH_2 molecule. The closed-shell singlet corresponds to qubit register S2 from in Table 1, while the open-shell singlet corresponds to qubit register S3 in Table 1. The circuits act on the fifth, sixth, seventh and eighth qubits of the register.

matches faithfully the one obtained with FCI, as shown in Figure 2 alongside the energy curve for the singlet ground state.

We study now the H_3 molecule with linear geometry and a 6-31G basis set. Here, we track the variation in energy with respect to the stretching of one H-H bond along the molecular axis. The spin states considered are the doublet (ground state with one unpaired electron) and the quadruplet (excited state with three unpaired electrons). Initialized qubit registers are shown in Table 1 for these spin multiplets. As in the H_2 case, the agreement between the VQE results and the FCI and CCSD results is almost perfect at all distances considered (see Figure 2). An extension of this study to the cation H_3^+ in its singlet and triplet curves displays similar accuracy. No crossover is observed between energy curves in any of the states studied.

3.2 VQE results for CH_2

We study the energy curves calculated with VQE for the symmetric stretching of both C-H bonds, fixing the H-C-H angle to 135° , as shown schematically in Figure 3. The ground state of CH_2 is a spin triplet with symmetry \tilde{X}^3B_1 whose main configuration is:

$$\tilde{X}^3B_1 \simeq (1a_1)^2(2a_1)^2(1b_2)^2(3a_1)^1(1b_1)^1 \quad (1)$$

This configuration is shown in Figure 3. One can see that the highest occupied molecular orbital is doubly degenerate. The first excited state of this molecule is a closed shell singlet with multireference character and symmetry \tilde{a}^1A_1 . A good description of this state is provided by the leading term:

$$\tilde{a}^1A_1 \simeq \lambda(1a_1)^2(2a_1)^2(1b_2)^2(3a_1)^2 - \sqrt{1-\lambda}(1a_1)^2(2a_1)^2(1b_2)^2(1b_1)^2 \quad (2)$$

where λ is a parameter that depends on the H-C-H angle of the molecule. The second excited singlet state is an open-shell singlet with symmetry \tilde{b}^1B_1 :

$$\tilde{b}^1B_1 \simeq (1a_1)^2(2a_1)^2(1b_2)^2(3a_1)^1\alpha(1b_1)^1\beta - (1a_1)^2(2a_1)^2(1b_2)^2(3a_1)^1\beta(1b_1)^1\alpha, \quad (3)$$

while the third lowest excited state is the closed-shell singlet \tilde{c}^1A_1 , which can be understood as a double excitation of the \tilde{a}^1A_1 singlet state:

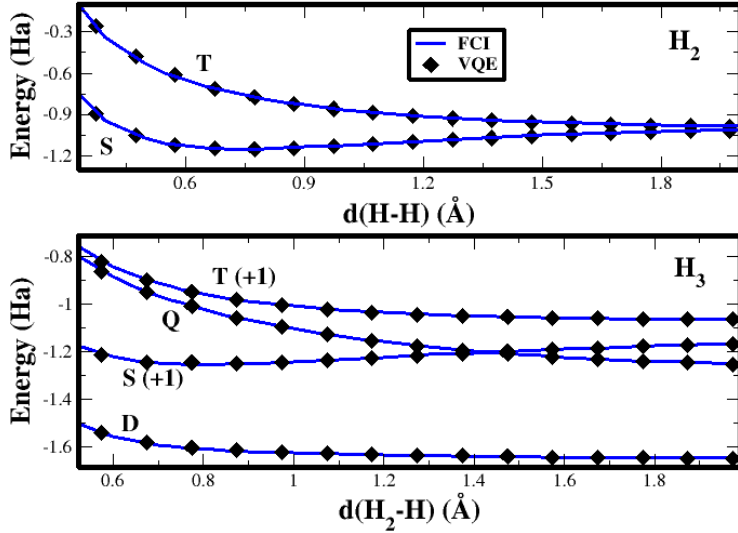


Figure 2: Energy curves for the elongation of a H-H bond in H_2 (top graph) and linear H_3 (bottom graph) at different spin states and charge states using VQE, compared with classical FCI results. Singlet (S) and triplet (T) curves have been considered for H_2 . In the case of H_3 , states considered are doublet (D), quadruplet (Q), cation singlet (S+1) and cation triplet (T+1).

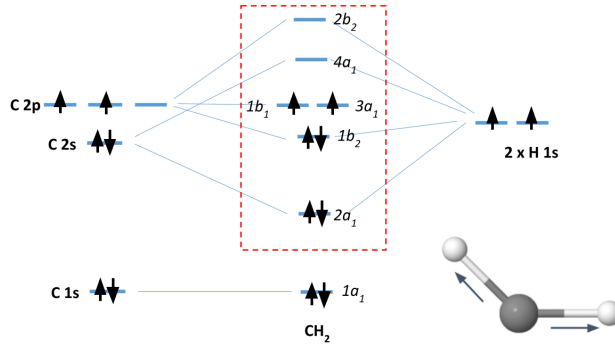


Figure 3: Geometry and molecular orbital diagram for CH_2 in the ground state (triplet symmetry). The active space used in this work is indicated as the set of orbitals inside the red box.

$$\tilde{c}^1 A_1 \simeq \lambda(1a_1)^2(2a_1)^2(1b_2)^2(1b_1)^2 + \sqrt{1-\lambda}(1a_1)^2(2a_1)^2(1b_2)^2(3a_1)^2 \quad (4)$$

This ordering of the excited states has been reported in previous works on CH_2 [25, 26], and is also observed from classically computed FCI and equation of motion coupled cluster (EOM-CC) energies. We have calculated energy curves for all these states using FCI and EOM-CC classical methods in order to use them as useful benchmarks for our VQE results. We now analyze the results obtained for each initial qubit register with different methods. Results for the ground and excited states of CH_2 are shown in figure 5.

3.2.1 Triplet ground state calculation

With the molecular integrals and qubit register for the initial ansatz set to the ground state triplet \tilde{X}^3B_1 (qubit register T in table 1), the FCI ground state energy was recovered by the VQE algorithm using the UCCSD and UCCGSD cluster operators. For the k -UpCCGSD calculations, the ground state \tilde{X}^3B_1 energy at the equilibrium geometry was calculated as a function of k up to $k = 3$. As shown in figure 4, when the k -UpCCGSD ansatz is adopted, variations of approximately

0.02 Ha in the optimized energy of \tilde{X}^3B_1 were observed when $k > 1$. It should be noted that the optimization procedure, which variationally optimizes the cluster amplitudes, begins with a randomization in which the initial amplitudes are Gaussian-distributed about 0 with a variance r_f . By plotting the optimized energies as a function of k for repeated runs with a range of variances $r_f = 1 \times 10^{-5} - 1 \times 10^{-2}$, a spread in the optimized energies for $k > 1$ is observed. The spread depends on r_f , with lower energies (closer to the FCI energy) obtained for larger values of r_f which permit sufficient variational flexibility for the k -UpCCGSD ansatz to approach the FCI limit.

This spread in energies for \tilde{X}^3B_1 using k -UpCCGSD is associated with the presence of many unphysical local minima, which in turn can arise from the fact that k -UpCCGSD energies are not invariant to unitary rotations of the spin orbitals [10]. Hence, we follow the approach of Lee *et al* [10] and use the lowest energy solutions for the ground state. A decrease in the ground state energy (at the minimum of the PES) of 0.015 Ha is observed between $k = 1$ and $k = 2$. For the latter, the lowest energy solution matches that for $k = 3$. This variation in ground state energy with respect to k is in qualitative agreement with the calculations reported by Lee *et al* [10], who observed convergence with respect to k for $k = 2$ to within a few mHa for ground states calculated at the potential energy surface (PES) minimum using the minimal basis set STO-3G. Thus, for the k -UpCCGSD calculations of the PES for ground and excited states of CH₂ we proceed with a maximum value of 2 for k , while also presenting the results for $k = 1$ for comparison, and adopt the randomization factor $r_f = 1 \times 10^{-2}$. Figure 5 shows that the \tilde{X}^3B_1 energy is 0.02 Ha above the FCI limit near the minimum of the PES for $k = 1$, hence k -UpCCGSD is within 6 mHa of the FCI limit for the ground state when $k = 2$.

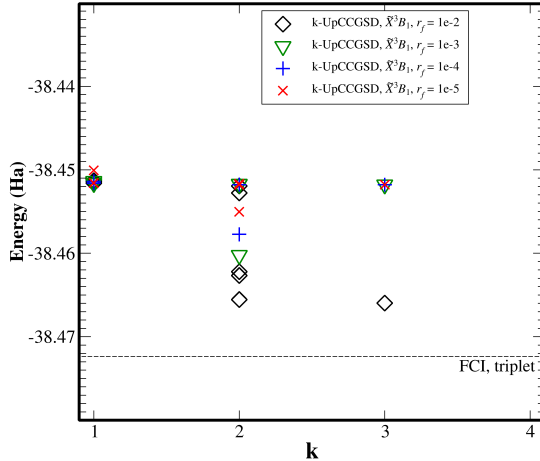


Figure 4: Energy versus k in k -UpCCGSD applied to the triplet ground state of CH₂. The dashed line denotes the FCI energy. For $k > 1$, a spread in energies reached at the end of optimization is observed which depends on the variance of the initially randomized cluster amplitudes, given by the randomization factor r_f .

3.2.2 Singlet excited states calculation

We focus now on the qubit registers encoding singlet functions, as the triplet ground state is well reproduced by CCSD, UCCSD, UCCGSD, and reasonably well for 2-UpCCGSD. Applying the UCCSD excitation operator to the S1 initial qubit register reproduces the FCI energy for the first excited state (\tilde{a}^1A_1) throughout the PES curve. This result is in striking contrast with conventional CCSD calculations on a classical machine, which fail to obtain the \tilde{a}^1A_1 state near the equilibrium geometry and converge instead to the \tilde{c}^1A_1 state, as shown in Figure 5. For the multireference S2 and S3 singlet registers, we resort to the k -UpCCGSD and UCCGSD cluster operators, and also apply these operators to the S1 register for comparison. The results of these calculations are presented in Figure 6. We first discuss the cases of S1 and S2. In some of these calculations, we obtain a lowering of the energy towards that of the ground state. In order to understand this behaviour, we performed an analysis of the expectation value of the total spin operator with respect to the optimized wavefunction $\langle \Psi | S^2 | \Psi \rangle$ for these states. In particular, for k -UpCCGSD applied to the S1 qubit register, values of $\langle \Psi | S^2 | \Psi \rangle = 1$ and $\langle \Psi | S^2 | \Psi \rangle = 2$ were observed for $k = 1$ and $k =$

2 respectively, after optimization, indicating a mixture of singlet and triplet states and a crossover to the ground state triplet, respectively. When k -UpCCGSD is applied to S2, no spin crossover ($\langle \Psi | S^2 | \Psi \rangle = 0$) is observed for 1-UpCCGSD, while for 2-UpCCGSD the total spin expectation value is consistent with a triplet ($\langle \Psi | S^2 | \Psi \rangle = 2$) and the ground state \tilde{X}^3B_1 energy is reproduced. Interestingly, for UCCGSD the effect of spin crossover towards the triplet only occurs when the initial state is prepared with the S1 register, whereas the S2 register retains its spin symmetry after VQE optimization routine using UCCGSD. Thus, using a multireference initial wavefunction is sufficient to prevent spin crossover in UCCGSD and recover the FCI limit of the first excited state. On the other hand, our results indicate the susceptibility of the k -UpCCGSD ansatz to spin crossover for the closed shell single reference and multireference states. Thus, comparing the excited state calculations between k -UpCCGSD and UCCGSD it is observed that restricting double excitations to spin pairs in the same spatial orbital while retaining generalized single excitations (as is adopted for k -UpCCGSD) can lead to energy states which do not retain the spin symmetry of the target state, when closed shell (single- or multireference) configurations are used. Inspection of the wavefunction in the crossover cases shows that the optimization process sometimes induces a change of sign in several leading amplitudes corresponding to single excitations from doubly occupied orbitals. These excitations drive the wavefunction to the $S_z = 0$ component of the triplet state and produce the spin switching. These findings are summarized in Table 2, which presents the observations of spin crossover (or lack thereof) for the various unitary cluster operators.

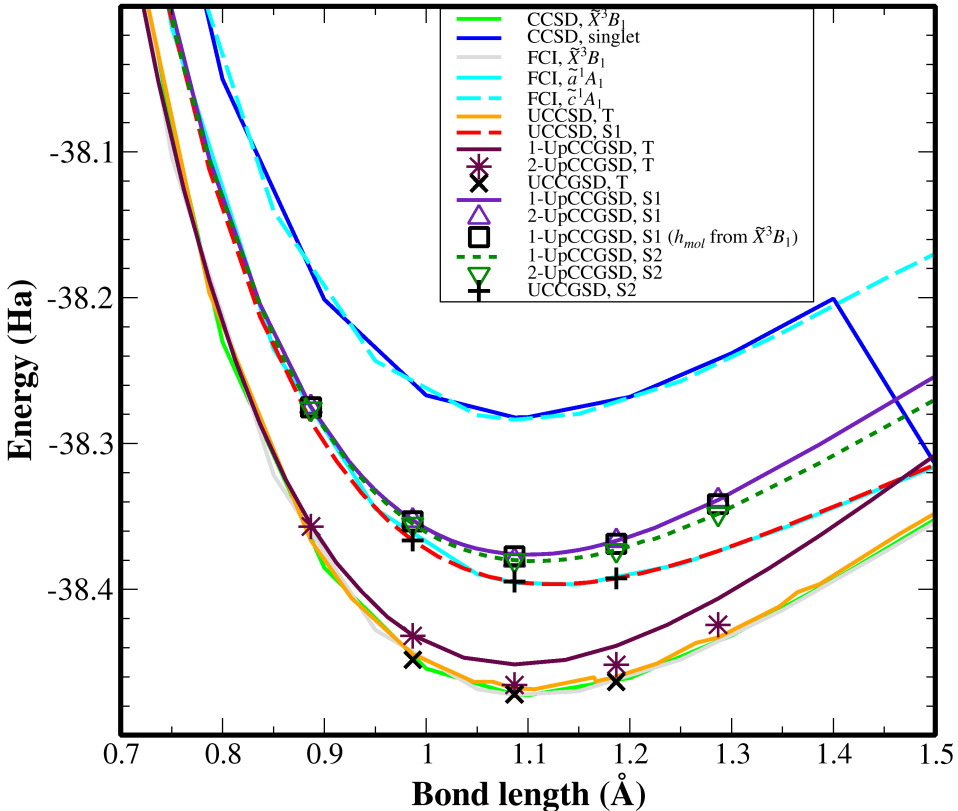


Figure 5: Energy versus C-H bond length (PES) curves for the ground and excited states of CH_2 , calculated using various representations of the cluster operator, and using different initial configurations of spin orbitals as input to VQE optimization. For k -UpCCGSD, solid lines denote results for $k = 1$, while the symbols of the corresponding color refer to results for $k = 2$. The black \times and $+$ symbols refer to the initial state configurations T and S2 (used for the \tilde{X}^3B_1 and \tilde{a}^1A_1 states) respectively, calculated using UCCGSD. The black \square symbols refer to the calculation in which the molecular wavefunction ansatz was set to a singlet, while the molecular Hamiltonian was set to the triplet.

To eliminate spin crossover to the triplet for the singlet registers in which it is observed, we follow the approach of constrained VQE optimization and restrict the Hilbert space dimension such that only states of a particular symmetry are considered [3]. By including a constraining term in the energy function E_{VQE} that is optimized,

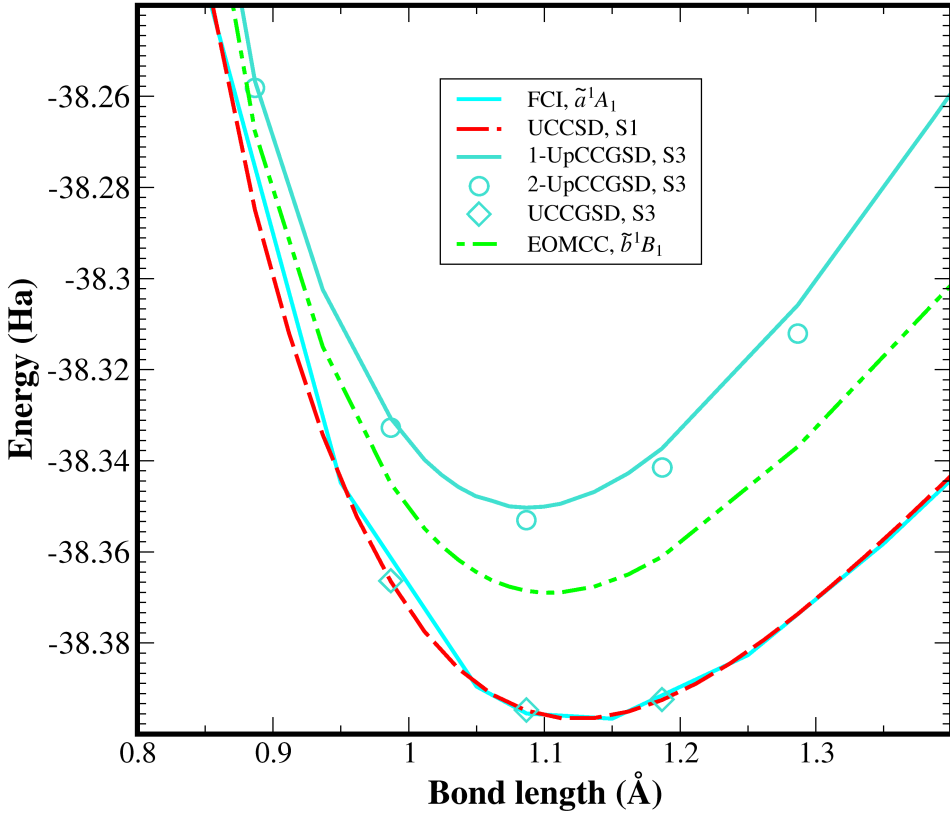


Figure 6: Energy versus C-H bond length (PES) curves for the excited singlet states of CH_2 using the S3 qubit register, calculated using various representations of the cluster operator. For k -UpCCGSD, the solid turquoise line denotes $k = 1$, while the turquoise \circ symbols refer to results for $k = 2$. Singlet classical curves and results using the S1 register are also included for comparison.

$$E_{VQE} = E + p |\langle \Psi | S^2 | \Psi \rangle|^2 \quad (5)$$

where p is a penalty factor, energies corresponding to the excited state singlet spin symmetry ($S^2 = 0$) can be calculated for all values of k and for the fully generalized operator. We adopt this approach to calculate the energy as a function of bond length using the k -UpCCGSD and UCCGSD operators applied to the qubit registers S1 and S2.

Once the symmetry constraints are applied, the UCCGSD closed shell singlet energies accurately follow the FCI singlet curve. For the constrained k -UpCCGSD energy, the value of k has a lower effect on the optimized energies throughout the PES than the \tilde{X}^3B_1 ground state. Compared to the UCCGSD operator, k -UpCCGSD performs slightly worse for the excited singlet states. At the PES minimum, the singlet calculated with the S1 register is 0.02 Ha above the FCI limit for $k = 1$, while this difference decreases to 0.016 Ha for $k = 2$. Essentially the same performance compared to FCI is observed for the curve calculated with the S2 register within k -UpCCGSD, however this limit is now reached for $k = 1$, with $k = 2$ yielding the same PES minimum energy to within 1 mHa. We attribute the relatively poor accuracy of k -UpCCGSD to the presence of two molecular bonds stretching simultaneously: this is one of the situations in which this ansatz is supposed to struggle to find accurate results [10].

We proceed now to study qubit register S3, which should represent the energy surface of the open shell multireference singlet \tilde{b}^1B_1 . The initial qubit register was prepared using the quantum circuit displayed on the bottom panel of Figure 1, and the cluster operators 1-UpCCGSD, 2-UpCCGSD, and UCCGSD were applied to it. For 2-UpCCGSD, five points around the minimum of the PES were calculated, while for UCCGSD only 3 points were calculated due to computational expense. These results were compared with the \tilde{b}^1B_1 curve obtained by classical EOMCC calculations. The 1-UpCCGSD and 2-UpCCGSD ansätze manage to conserve the \tilde{b}^1B_1 character of the wavefunction, but tend to overestimate the energy of this state relative to EOMCC, as shown in

Table 2: Qubit registers encoding the initial ansatz, and the resulting symmetry of the state following VQE optimization using various unitary cluster operators, without the application of spin symmetry constraints. No UCCSD results for registers S2 and S3 are included, as this operator is not suited for multireference states. A mixing of the singlet and triplet states (\tilde{a}^1A_1 / \tilde{X}^3B_1) is observed when the 1-UpCCGSD operator is applied to the S1 qubit register, indicating spin contamination in this case.

<i>initial qubit register</i>	UCCSD	1-UpCCGSD	2-UpCCGSD	UCCGSD
S1	\tilde{a}^1A_1	\tilde{a}^1A_1 / \tilde{X}^3B_1	\tilde{X}^3B_1	\tilde{X}^3B_1
S2		\tilde{a}^1A_1	\tilde{X}^3B_1	\tilde{a}^1A_1
S3		\tilde{b}^1B_1	\tilde{b}^1B_1	\tilde{a}^1A_1

figure 6. In contrast, we find that the UCCGSD ansatz calculation converges to the closed shell singlet \tilde{a}^1A_1 . The latter result is in fact not unexpected as the fully generalized UCCGSD operator should indeed converge to the variational minimum for a given symmetry. No spin crossover is observed for any of the ansätze applied to the S3 register (hence a penalty constraint is not applied for this case, as reported in table 2). This is at variance to the closed shell single reference (S1) or multireference (S2) cases. Further studies are required to understand these aspects of the various cluster operators and qubit register representations of the singlets, and this will be explored in a future work.

To conclude this section, our results show that generalized cluster operators lead to a strong dependence of the performance of the VQE algorithm (i.e. whether the algorithm can reach the desired solution) on the symmetry properties of the initialized state (single reference or multireference, closed-shell or open-shell). In general, for the VQE algorithm both the initial wavefunction ansatz $|\Psi_0\rangle = U_0|\text{HF}\rangle$ and the orbitals that enter the one- and two-electron (Hartree-Fock) integrals for the second quantization Hamiltonian h_{mol} (given as input to the optimization routine) usually share the same spin symmetry. Here, U_0 represents the unitary cluster operator in which the excitation amplitudes have their initially randomized values. To further investigate the dependence of the VQE algorithm on the initial state, a test was carried out to qualitatively check the relative contributions of $|\Psi_0\rangle$ and h_{mol} to the VQE-calculated total energy. To this end, $|\Psi_0\rangle$ was initialized to a closed shell singlet (via circuit preparation for $|\text{HF}\rangle$), while the integrals in h_{mol} were obtained from a Hartree-Fock calculation with the molecular orbitals arranged in a spin triplet. This test was performed for a range of C-H bond lengths around the PES minimum using 1-UpCCGSD, and the results are shown as the black \square symbols in figure 5. As can be seen, the optimized energies correspond very closely to the singlet excited state for the same cluster operator. Moreover, the initial (unoptimized) energy for this calculation is only 3 mHa above that of the initial energy when the singlet configuration is used for $|\Psi_0\rangle$ and h_{mol} . These results strongly indicate that the initial wavefunction ansatz is by far the stronger contributor to the total energy calculated from the VQE procedure.

3.2.3 Charged states calculation

k -UpCCGSD calculations were also performed for the anionic (CH_2^-) and cationic (CH_2^+) states of CH_2 . At the minimum of the PES curves the CH_2^- and CH_2^+ ground states correspond to spin doublets with energies of -38.1498 Ha and -38.1453 Ha, respectively for $k = 1$. For $k = 2$, the minimum total energy for CH_2^- (CH_2^+) is lowered by 0.005 Ha (0.008 Ha) relative to $k = 1$. When UCCSD is adopted, the FCI limit for the charged states is recovered. It is interesting to note that the ionic states remain separated from the neutral single reference and multireference singlet states by a large amount throughout the PES curve; at the minima both ionic states have energies approximately 0.22-0.23 Ha above that of the single reference singlet, when comparing results from UCCSD calculations. Thus, these calculations show that the neutral singlet state is not accessed by either charged ionic doublet via unconstrained VQE optimization.

Table 3: Optimized amplitudes for generalized excitations obtained with k -UpCCGSD ($k = 1, 2, 3$) and UCCGSD, for the triplet (\tilde{X}^3B_1) ground state of CH_2 , categorized by single and double excitations. The weight of each excitation is given as a percentage of the total sum of coefficients in the cluster operator. Indices a, b, c, d refer to occupied spatial orbitals, while p, q, r, s denote virtual spatial orbitals. For each value of k , the lowest energy solution is used.

$k = 1$	excitation	% weight
	t_a^p	7.34
<i>singles</i>	t_a^b	1.52
	t_p^q	1.19
	$t_{a,a}^{p,p}$	48.62
<i>doubles</i>	$t_{a,a}^{b,b}$	33.85
	$t_{p,p}^{q,q}$	7.49
$k = 2$		
	t_a^p	10.73
<i>singles</i>	t_a^b	29.68
	t_p^q	23.75
	$t_{a,a}^{p,p}$	10.90
<i>doubles</i>	$t_{a,a}^{b,b}$	12.86
	$t_{p,p}^{q,q}$	12.08
$k = 3$		
	t_a^p	17.61
<i>singles</i>	t_a^b	50.41
	t_p^q	14.20
	$t_{a,a}^{p,p}$	10.78
<i>doubles</i>	$t_{a,a}^{b,b}$	5.80
	$t_{p,p}^{q,q}$	1.20
UCCGSD		
	t_a^p	12.46
<i>singles</i>	t_a^b	1.01
	t_p^q	0.52
	$t_{a,b}^{p,q}$	37.35
	$t_{a,b}^{c,d}$	1.01
<i>doubles</i>	$t_{p,q}^{r,s}$	0.78
	$t_{a,p}^{b,q}$	3.79
	$t_{a,b}^{c,p}$	26.85
	$t_{a,p}^{q,r}$	16.24

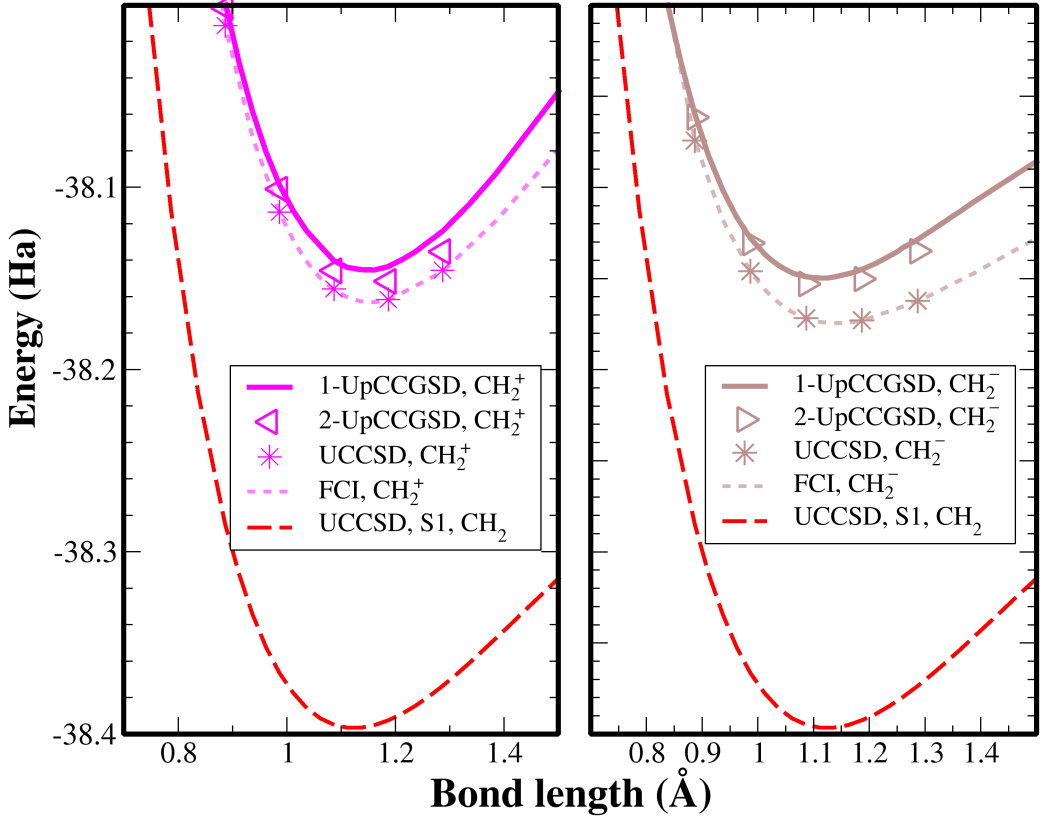


Figure 7: Energy versus C-H bond length (PES) curves for charged molecules CH_2^+ (left panel) and CH_2^- (right panel) calculated using the UCCSD and 1-UpCCSD cluster operators. These are also compared to classical calculations and the UCCSD calculation of the $\tilde{\alpha}^1A_1$ neutral state.

4 Discussion

In general, our results for the molecules considered in this study show that VQE is capable of calculating excited and ionic states, provided their spin or particle number symmetry is different from that of the ground state. A recently published article [16] has reported results for various excited states of H_2 using constrained VQE with a hardware efficient form of the trial wavefunction ansatz [32]. The authors propose that VQE calculations may suffer from convergence to unwanted states due to a lack of constraints which cause VQE optimization to tend toward energy states of different symmetry than the ground state of interest, as these states may be lower in energy at certain regions of the PES. Our calculations of the PES curves of excited and ionic states for H_2 , H_3 and CH_2 using the UCCSD ansatz and a qubit register representing a Hartree-Fock wavefunction rule this out as a general property of VQE, as no crossover to lower energy states is observed. In fact, by allowing the preparation of the mean-field (e.g. Hartree-Fock) state to be variationally optimized (using parameterized $R_X(\theta)$ rotation gates), we can reproduce the transition from the neutral triplet to the cation doublet reported at Ref [16], and observe the "kink" at bond length ~ 0.7 Å, for H_2 . This transition does not occur, and no switching between states is observed for the molecules considered when the Hartree-Fock state is prepared by non-parameterized gates which flip the desired number of qubits to correspond to the desired number of occupied spin orbitals (e.g. X gates). This shows that the ansatz proposed in ref. [32] can lead to unexpected instabilities during a VQE calculation, and additional symmetry constraints may need to be considered when parameterizing qubit rotations which prepare the mean-field state. Our calculations show, however, that the generalized UCCGSD and k -UpCCGSD ansätze do require additional constraints to obtain the correct PES in some cases, as shown in our CH_2 singlet calculations. It is not obvious at first glance whether a calculation using these ansätze will give the correct energy surface at certain set of symmetries, and this constitutes a strong argument to combine them with symmetry-constraining methods to ensure that the correct results are achieved.

The results presented above indicate the importance of the initial state preparation for VQE. The results for different CH_2 singlet qubit registers also emphasize the importance of the initial

configuration, where it is shown that the S3 open shell singlet register may drive the wavefunction to the \tilde{b}^1B_1 state for some of the ansätze considered, albeit with low accuracy in the energy values. Also, when VQE optimization is performed in the presence of multiple local minima near the optimal solution, careful examination of the initial state and its evolution during optimization is necessary, and possibly optimization constraints need to be imposed, for the algorithm to reach the correct energy surface. A representative case is the set of CH_2 calculations with the k -UpCCGSD ansatz performed in this work. For the triplet state, small differences of approximately 1.5 mHa in the optimized energy were observed for $k = 1$ as a function of initial cluster amplitude randomization. These energy differences are proportional to differences in the set of optimized cluster amplitudes, with the 1.5 mHa difference being accounted for by variations in amplitudes involving occupied-virtual and virtual-virtual double excitations. For the spread of 0.02 Ha in the energy of the ground state observed for calculations with $k > 1$, again virtual-virtual transitions play a role in the energy difference, however large variations in occupied-occupied single and double excitations are also observed, with the lowest energy solutions including occupied-occupied singles transitions which have very small amplitudes in the cases of higher total energy. The % weights of each type of excitation for the triplet ground state within k -UpCCGSD are shown in table 3, where the lowest energy solutions from figure 4 are used for each value of k . The excitation weights are also shown for UCCGSD. The UCCGSD approach exhibits a large re-balancing of spectral weights relative to k -UpCCGSD. In particular, the large weight of the generalized single excitations in 3-UpCCGSD are redistributed to the generalized doubles of UCCGSD. Note that the latter reproduces the FCI limit of the ground state energy to within 1 mHa, thanks to the inclusion of double excitations of spin orbitals in different spatial orbitals. This comparison explains the observed variation in accuracy of the k -UpCCGSD approach applied to the ground state; the greater degree of variational flexibility associated with larger values of k allows for a partial compensation for the lack of generalized doubles in k -UpCCGSD, resulting in a large transfer of spectral weight to the fully generalized singles (occupied-occupied transitions in this case) in order to achieve solutions closer to the FCI ground state. Similar results are obtained in the singlet case. These results show how insufficient variational freedom in the excitation amplitudes (i.e. 1-UpCCGSD for \tilde{X}^3B_1), or neglecting generalized double excitations (1-UpCCGSD and 2-UpCCGSD for \tilde{a}^1A_1) in the cluster operator can result in inaccurate ground and excited state energies, respectively, for CH_2 and for complex molecules in general.

5 Conclusions

In conclusion, VQE calculations using various representations of the unitary cluster operator have been performed for the molecules H_2 , H_3 , and CH_2 , with different choices for the spin symmetry and number of electrons encoded in the qubit register. In the case of H_2 and H_3 , the UCCSD energy curves obtained for each symmetry accurately match the expected results from calculations on classical machines at a similar level of theory.

CH_2 corresponds to a particularly interesting case to assess the performance of different VQE ansätze due to the presence of non-trivial contributions of electronic correlation to the ground and excited states. We find that while UCCSD, UCCGSD, and spin-paired 2-UpCCGSD all reproduce well the energy of the triplet ground state, the first singlet excited state is only accurately reproduced by the UCCSD ansatz. Generalized ansätze require either initial qubit registers with multireference character or the application of symmetry constraints in order to quantitatively reproduce this state. Efforts to drive VQE to obtain the second singlet excited state of CH_2 by setting the initial qubit register to an appropriate multireference open-shell state fail for either UCCSD or UCCGSD; however, k -UpCCGSD manages to obtain a wavefunction of the correct symmetry, although with a significant overestimation of the energy associated to this state.

At variance to the conclusions reached by Ryabinkin et al [16], excited states can indeed be accessed by VQE with the UCCSD ansatz without imposing penalty constraints in the objective function, as long as the parameters (qubit rotations applied to the initial qubit register) for mean-field state preparation are fixed during variational optimization of the cluster amplitudes. While fixing the mean-field state preparation can itself be viewed as a constraint, this is a constraint that is imposed by knowledge of the electronic structure of the problem of interest. Hardware efficient ansätze which provide increased variational freedom while improving computational efficiency need to be used with caution, as these ansätze may introduce the possibility of different (undesired) Hilbert spaces being traversed during optimization. As previously described, similar

care has to be taken when using generalized coupled cluster operators. Again, the dependency of the VQE algorithm on the initial configuration is emphasized.

The results presented in this article demonstrate that VQE may be used to calculate excited states, provided they display different symmetry to that of the molecular ground state. They also show the importance of testing VQE ansätze on molecules or other systems with sufficient complexity, preferably beyond simple toy models. In particular, for studying many-body electronic systems using different approximations developed to balance efficiency with accuracy, clearly only systems with sufficient electronic correlation can test the full extent of the (in)adequacies of these approximations.

6 Acknowledgements

We would like to acknowledge useful discussions with Dr. Yu-ya Ohnishi from JSR Corporation (Japan).

References

- (1) Preskill, J. Quantum Computing in the NISQ era and beyond. *Quantum* **2018**, *2*, 79.
- (2) McClean, J. R.; Kimchi-Schwartz, M. E.; Carter, J.; de Jong, W. A. Hybrid quantum-classical hierarchy for mitigation of decoherence and determination of excited states. *Phys. Rev. A* **2017**, *95*, 042308.
- (3) Higgott, O.; Wang, D.; Brierley, S. Variational Quantum Computation of Excited States. *Quantum* **2019**, *3*, 156.
- (4) Parrish, R. M.; Hohenstein, E. G.; McMahon, P. L.; Martinez, T. D. Quantum Computation of Electronic Transitions Using a Variational Quantum Eigensolver. *Phys. Rev. Lett.* **2019**, *122*, 230401.
- (5) Veis, L.; Pittner, J. Quantum computing applied to calculations of molecular energies: CH₂ benchmark. *J. Chem. Phys.* **2010**, *133*, 194106.
- (6) O'Brien, T. E.; Senjean, B.; Sagastizabal, R.; Bonet-Monroig, X.; Dutkiewicz, A.; Buda, F.; DiCarlo, L.; Visscher, L. Calculating energy derivatives for quantum chemistry on a quantum computer. *arXiv:1905.03742[quant-ph]*, **2019**.
- (7) Mitarai, K.; Nagakawa, Y. O.; Mizukami, W. Theory of analytical energy derivatives for the variational quantum eigensolver. *arXiv:1905.04054[quant-ph]*, **2019**.
- (8) Parrish, R. M.; Hohenstein, E. G.; McMahon, P. L.; Martinez, T. D. Hybrid Quantum/Classical Derivative Theory: Analytical Gradients and Excited-State Dynamics for the Multistate Contracted Variational Quantum Eigensolver. *arXiv:1906.08728[quant-ph]*, **2019**.
- (9) Peruzzo, A.; McClean, J.; Shadbolt, P.; Yung, M.-H.; Zhour, X.-Q.; Love, P. J.; Aspuru-Guzik, A.; O'Brien, J. L. A variational eigenvalue solver on a photonic quantum processor. *Nature Communications* **2014**, *5*, 4213.
- (10) Lee, J.; Huggins, W. J.; Head-Gordon, M.; Birgitta Whaley, K. Generalized Unitary Coupled Cluster Wavefunctions for Quantum Computation. *J. Chem. Theory Comput.* **2019**, *15*, 311.
- (11) Grimsley, H. R.; Economou, S. E.; Barnes, E.; Mayhall, N. J. An adaptive variational algorithm for exact molecular simulations on a quantum computer. *Nature Comms.* **2019**, *10*, 3007.
- (12) Bauman, N. P.; Bylaska, E. J.; Krishnamoorthy, S.; Low, G. H.; Wiebe, N.; Granade, C. E.; Roetteler, M.; Troyer, M.; Kowalski, K. Downfolding of many-body Hamiltonians using active-space models: Extension of the sub-system embedding sub-algebras approach to unitary coupled cluster formalisms. *J. Chem. Phys.* **2019**, *151*, 014107.
- (13) Motta, M.; Ye, E.; McClean, J. R.; Li, Z.; Minnich, A. J.; Babbush, R.; Chan, G. K.-L. Low rank representations for quantum simulation of electronic structure. **2018**.
- (14) Ryabinkin, I. G.; Yen, T.-C.; Genin, S. N.; Izmaylov, A. F. Qubit Coupled Cluster Method: A Systematic Approach to Quantum Chemistry on a Quantum Computer. *J. Chem. Theory Comput.* **2018**, *14*, 6317.

(15) McArdle, S.; Yuan, X.; Benjamin, S. Error-Mitigated Digital Quantum Simulation. *Phys. Rev. Lett.* **2019**, *122*, 180501.

(16) Ryabinkin, I. G.; Genin, S. N.; Izmaylov, A. F. Constrained Variational Quantum Eigensolver: Quantum Computer Search Engine in the Fock Space. *J. Chem. Theory Comput.* **2019**, *15*, 249.

(17) scikit-quant. Optimizers for Noisy Intermediate-Scale Quantum devices., <https://qat4chem.lbl.gov/software>, 2019.

(18) Izmaylov, A. F.; Yenab, T.-C.; Ryabinkin, I. G. Revising the measurement process in the variational quantum eigensolver: is it possible to reduce the number of separately measured operators? . *Chem. Sci.* **2019**, *10*, 3746.

(19) Wang, D.; Higgott, O.; Brierley, S. *Phys. Rev. Lett.* **2018**, *122*, 140504.

(20) Cao, Y.; Romero, J.; Olson, J. P.; Degroote, M.; Johnson, P. D.; Kieferova, M.; Kivlichan, I. D.; Menke, T.; Peropadre, B.; Sawaya, N. P. D.; Sim, S.; Veis, L.; Aspuru-Guzik, A. Quantum Chemistry in the Age of Quantum Computing. *arXiv:1812.09976[quant-ph]*, **2018**.

(21) McArdle, S.; Endo, S.; Aspuru-Guzik, A.; Benjamin, S.; Yuan, X. Quantum Computational Chemistry. *arXiv:1808.10402[quant-ph]*, **2019**.

(22) Gao, Q.; Nakamura, H.; Gujarati, T. P.; Jones, G. O.; Rice, J. E.; Wood, S. P.; Pistoia, M.; Garcia, J. M.; Yamamoto, N. Computational Investigations of the Lithium Superoxide Dimer Rearrangement on Noisy Quantum Devices. *arXiv:1906.10675*, **2019**.

(23) Szalay, P. G.; Müller, T.; Gidofalvi, G.; Lischka, H.; Shepard, R. Multiconfiguration Self-Consistent Field and Multireference Configuration Interaction Methods and Applications. *Chem. Rev.* **2012**, *112*, 108.

(24) Bartlett, R. J.; Musiał, M. Coupled-cluster theory in quantum chemistry. *Rev. Mod. Phys.* **2007**, *79*, 291.

(25) Green, W. H.; Handy, N. C.; Knowles, P. J.; Carter, S. Theoretical assignment of the visible spectrum of singlet methylene. *J. Chem. Phys.* **1991**, *94*, 118.

(26) Slipchenko, L. V.; Krylov, A. I. Singlet-triplet gaps in diradicals by the spin-flip approach: A benchmark study. *J. Chem. Phys.* **2002**, *117*, 4694.

(27) Veis, L.; Pittner, J. Adiabatic state preparation study of methylene. *J. Chem. Phys.* **2014**, *140*, 214111.

(28) Steiger, D. S.; Häner, T.; Troyer, M. ProjectQ: An Open Source Software Framework for Quantum Computing. *Quantum* **2018**, *2*, 49.

(29) McClean, J. R. et al. OpenFermion: The Electronic Structure Package for Quantum Computers. *arXiv:1710.07629[quant-ph]*, **2017**.

(30) Parrish, R. M. et al. Psi4 1.1: An Open-Source Electronic Structure Program Emphasizing Automation, Advanced Libraries, and Interoperability. *J. Chem. Theory Comput.* **2017**, *13*(7), 3185.

(31) Bravyi, S. B.; Kitaev, A. Y. Fermionic Quantum Computation. *Ann. Physics* **2000**, *298*, 210.

(32) Kandala, A.; Mezzacapo, A.; Temme, K.; Takita, M.; Brink, M.; Chow, J.; Gambetta, J. Hardware-efficient variational quantum eigensolver for small molecules and quantum magnets. *Nature* **2017**, *549*, 242.